



Study on adsorption of phosphorus by modified aluminum-based drinking water treatment sludge

Zhenhua Qin, Jiuhong Yu, Ken Chen, Guozhi Fan, Qunpeng Cheng*, Guangsen Song*

School of Chemical and Environmental Engineering, Wuhan Polytechnic University, Wuhan 430023, China, email: whpuchem@126.com (Z. Qin), 2711976109@qq.com (J. Yu), 523057945@qq.com (K. Chen), 6524677@qq.com (G. Fan), cqp627@126.com (Q. Cheng), 1697446119@qq.com (G. Song)

Received 4 September 2018; Accepted 25 February 2019

ABSTRACT

A modified drinking-water treatment sludge (MDWTS) by pyrolysis was used as the adsorbent for the removal of phosphorus. The influence of pyrolysis temperature, dosage of adsorbent, contact time and pH on the P adsorption capacity were tested. Meanwhile the equilibrium and kinetics of adsorption process by DWTS and MDWTS were also studied. The results showed that the adsorption capacity of DWTS was greatly improved after pyrolyzed. The increase of pyrolysis temperature was benefit for the phosphorus adsorption. The maximum adsorption capacity (25.32 mg/g) of MDWTS was appeared at 800°C. The adsorption capacity of DWTS and MDWTS was strongly dependent on solution pH especially at low pH. The maximum phosphorus adsorption capacity were achieved at pH 5. As the dosage of DWTS and MDWTS increased from 0.5 to 3 g/100 ml, P adsorption capacity decreased from 7.47 mg/g to 1.74 mg/g and 22.45 mg/g to 3.26 mg/g respectively. High-adsorbent dosage could effectively reduce the unsaturation of the ion-exchange sites of DWTS and MDWTS which caused comparatively lesser ion exchange. The adsorption isotherms of P removal by DWTS and MDWTS were well described by Freundlich models, suggesting the adsorption of phosphorus was a heterogeneous surface adsorption process. Meanwhile kinetics studies showed that the adsorption process of P followed pseudo-second order kinetic model.

Keywords: Drinking-water treatment sludge; Pyrolysis; Modified; Adsorption; Phosphorus

1. Introduction

Phosphorus (P) removal has been obtained much attentions as it will cause the eutrophication of water. P removal can be achieved by traditional chemical precipitation with aluminum [1], calcium and iron salts [2], physicochemical methods including reverse osmosis, electrodialysis, contact filtration and adsorption, and biological methods [3,4]. Among these methods, adsorption techniques are most popular ways by various adsorbents and bio-adsorbents such as activated aluminum oxide, zeolites [5], biochar, activated carbon and flyash [6].

Drinking-water treatment sludge (DWTS) is produced during the purification of drinking water, where the alumi-

num based salt is usually used as a coagulant to remove color, turbidity and humic substances [7]. The common disposals of DWTS are (1) directly discharged into water bodies, (2) disposed in land fill, (3) discharged into publicly owned treatment works [8]. Those disposals are not environmental and economical even they can produce the secondary pollution.

As a by-product generated, DWTS had been received increasing research interest in its resource utilization which could be used as the building material of brick, cement and ceramics, especially used as adsorbent [9–13]. The aluminum and iron ions contained in the DWTS made it potential for adsorption of phosphorus [14]. The ability of phosphorus adsorption capacity for two kinds of DWTS were investigated by Tie Jingxi. The results showed that the maximum

*Corresponding author.

phosphorus adsorption capacity of alum sludge and iron sludge were $12.5 \text{ mg}\cdot\text{g}^{-1}$ and $7.813 \text{ mg}\cdot\text{g}^{-1}$. High temperature, acid environment and low phosphorus concentration were favorable for enhancing phosphorus adsorption [15]. A phosphorus adsorption capacity of approximately $12.5 \text{ mg}\cdot\text{g}^{-1}$ and $37.0 \text{ mg}\cdot\text{g}^{-1}$ were achieved by Ippolito and Dayton [16,17]. The potential of aluminum-based water treatment residuals used as phosphorus-removing substrate in engineered wetlands were assessed by Babatunde. Batch tests obtained a maximum P adsorption capacity of $31.9 \text{ mg}\cdot\text{P}/\text{g}$ and significant P removal rate was achieved in column tests [18]. Overall, research results showed that DWTS could be used as a low-cost, easily available and effectively adsorbents for P removal.

However, during the flocculation process, the organic matter, bacteria and inorganic substances were removed by aluminum flocculant through adsorbing and changing the charge of the water colloid particle. These substances contained in DWTS may occupy the adsorption site which will restrict the adsorption capacity of sludge (DWTS) [19]. The objective of this study is to investigate the P adsorption behavior of modified DWTS (MDWTS) through pyrolysis. The influence of pyrolysis temperature, dosage of adsorbents, contact time and pH on the P adsorption capacity were tested. The equilibrium and kinetics of adsorption of P onto the DWTS and MDWTS were also studied.

2. Material and methods

2.1. Materials

The DWTS used in the experiment was taken from Zongguan drinking water plant in WuHan, HuBei province, China, which used polyaluminum ferric chloride (PAFC) as the coagulant. The obtained DWTS samples were first dried for 48 h under 105°C in a drying oven for the subsequent experiments.

2.2. Methods

In the pyrolysis experiment, DWTS was loaded in a combustion boat and put into a tube furnace pyrolyzed for 10 min. Nitrogen was served as the protect gas at a rate of about $1 \text{ L}/\text{min}$ which was passed over tube furnace in advance in order to clean up the air. The pyrolysis temperature ranged from 500 to 900°C . The retention time was maintained for 2 h. At last MDWTS were taken out after cooled down. The weight loss rate at various temperatures was calculated by Eq. (1):

$$\text{Weight loss rate} = \frac{\text{mass of sludge} - \text{mass of biochar}}{\text{mass of sludge}} \times 100\% \quad (1)$$

Artificial wastewater used in this study was synthesized by adding a certain amount of KH_2PO_4 into distilled water. The concentration of P ranged from 10 to $50 \text{ mg}/\text{L}$. In order to investigate the effect of pH on adsorption capacity, pH of the solution was increased from 5 – 9 which was adjust by NaOH and HCl. 0.1 – 0.5 g of either DWTS or MDWTS was placed into a 30 mL glass bottle. Subsequently, 30 mL artificial wastewater was added and intensively mixed using

a vortex maker. After stirring by a thermostatic box for 4 h at $25 \pm 1^\circ\text{C}$, the suspensions were filtered and the residual concentration of P in solutions was test.

pH value was determined using a Thermo (Shanghai, China) pH meter which was calibrated daily using pH buffer solution. Surface area and main chemical components of DWTS and MDWTS such as aluminum, silica and iron were measured by a Brunauer-Emmett-Teller/energy dispersive spectroscopy (BET/EDS). The mineral compositions were examined by X-ray diffractometer (XRD). The spectra of the samples were measured using Fourier transform infrared spectroscopy (FTIR, Nicolet 6700). The resulting spectra were normalized to the highest peak in the fingerprint region between 4000 and 400 cm^{-1} . Phosphorus concentration was determined by the colorimetric method. All of the tests were conducted in 3 replications, and the mean values were used. Scanning electron microscopy (SEM) was also inspect the structure of DWTS and MDWTS.

2.3. Adsorption isotherms model

In this study, adsorption isotherm was developed to describe the adsorption of DWTS and MDWTS by Langmuir and Freundlich model [Eqs. (2) and (3)].

$$\frac{C_e}{q_e} = \frac{1}{q_{\max} k_L} + \frac{C_e}{q_{\max}} \quad (2)$$

$$\log q_e = \log k_F + \frac{1}{n} \log C_e \quad (3)$$

where k_L and k_F is respectively represented for the Langmuir isotherm constant (L/mg) and Freundlich isotherm constant (mg/g). q_{\max} represents the maximum P uptake capacity of DWTS and MDWTS (mg/g). C_e is the equilibrium P concentration in the liquid phase (mg/L) and q_e is the mass of phosphorus adsorbed per unit mass of DWTS and MDWTS (mg/g). $1/n$ is the Freundlich isotherm constant which is dimensionless.

2.4. Regeneration of adsorbent

MDWTS after saturated with phosphorus by HNO_3 solution with different concentrations (0.1 , 0.5 , 1 and $1.5 \text{ mol}/\text{L}$) was first placed in a thermostatic oscillator for desorption reaction. After 24 h, it was washed with deionized water and dried. The recycled MDWTS was placed in a phosphorous solution with an initial concentration of $30 \text{ mg}/\text{L}$ for re-adsorption experiment. The adsorption performance of MDWTS on phosphorus after regeneration was determined and its regeneration efficiency was calculated by Eq. (4).

$$\eta = \frac{Q_e \text{ after regeneration}}{Q_e \text{ before regeneration}} \quad (4)$$

where η was the regeneration rate(%); $Q_e \text{ after regeneration}$ was the adsorption capacity of MDWTS after regeneration (mg/g); $Q_e \text{ before regeneration}$ was the adsorption capacity of MDWTS before adsorption (mg/g).

3. Results and discussion

3.1. Characteristics of DWTS and MDWTS

The chemical composition of DWTS and MDWTS determined by XRF is shown in Table 1. The main content of DWTS was SiO₂ which covered more than 55%. The content of aluminum (expressed as Al₂O₃) and iron (expressed as Fe₂O₃) ranged from 27.72%–32.18%. The properties of DWTS were highly variable which were dependent on both the type of the raw water and the chemical composition of coagulant. After pyrolysis, the content of SiO₂ and Al₂O₃ increased with the increase of pyrolysis temperature. The minimum SiO₂/Al₂O₃ ratio was obtained at 800°C. DWTS samples were composed of clay, humic substances, mental hydroxide, active carbon and coagulants. Humic substances (TOC) was decomposed after pyrolysis. As shown in Table 1, the content of SiO₂ increased from 52.6% to 58.3% with the increase of temperature, while heavy metals showed good stability during the pyrolysis process. Meanwhile, the weight loss rate increased from 11.20% at 500°C to 16.90% at 900°C which was because that more organic materials were decomposed at the higher temperature.

BET results of DWTS and MDWTS are shown in Table 2. The surface area and pore volume of the MDWTS decreased gradually with the increase of temperature after pyrolysis. At 500°C, an exception to the law on changes in surface area and pore volume versus pyrolysis temperature was observed. MDWTS500 with relatively small pores (compared with MDWTS600, MDWTS700, MDWTS800 and MDWTS900) had the largest surface area and pore volume. With the increase of pyrolysis temperature, the organic matters were decomposed and the evolution of secondary volatiles, gases bubbled out, the skeleton of sludge collapsed which caused the pore shrinking. Though the surface area and pore volume were decreased after pyrolysis, the adsorption capacity of MDWTS was better than DWTS in combination with the surface functional group distribution which could be verified in the latter experiments. The results suggested that surface complexation was not the main mechanism for P adsorption on the MDWTS.

Fig. 1 shows the SEM micrographs of DWTS and MDWTS. It can be observed that all the samples were composed by granular porous materials which was benefit for the adsorption. Meanwhile, With the increase of pyrolysis temperature, the number of mesoporous structures increased and some mesoporous structures of MDWTS

collapsed which aggravated the chaotic distribution of mesopores.

The FTIR analysis (Fig. 2) demonstrated that the character peaks of DWTS and MDWTS were similar which indicated that pyrolysis did not affect the structural formation of organic functional groups in DWTS. The peaks at 2800 cm⁻¹–3000 cm⁻¹, 980–1000 cm⁻¹ and 550 cm⁻¹–850 cm⁻¹ represented the C–H, C–OH and C–Cl [20–22]. Thus, DWTS and MDWTS were rich in organic functional groups such as C–H, C–OH and C–Cl which was benefit for P adsorption.

3.2. PO₄³⁻-P adsorption behavior

3.2.1. Phosphorus adsorption capacity

In order to establish equilibrium for adsorption and investigate the kinetic of the adsorption process, the relationship between initial concentration of P and the amount of P adsorbed per unit mass of DWTS and MDWTS is shown in Fig. 3. The results showed that the P adsorption capacity of DWTS could be greatly increased by pyrolysis. The maximum phosphorus adsorption capacity were 6.50 mg/g, 12.33 mg/g, 16.10 mg/g, 20.43 mg/g, 25.32 mg/g and 19.51 mg/g respectively for DWTS, MDWTS500, MDWTS600, MDWTS700, MDWTS800 and MDWTS900. The maximum P adsorption capacity (25.32 mg/g) was appeared at MDWTS800. Several adsorbents including slags (2.49 mg/g) [23], fly ash (13.47 mg/g) [24], magnesium modified corn biochar (16.6mg/g) [20] and zeolite (19.11 mg/g) [25] for P removal capacities had been reported. In comparison, the MDWTS used here could be seen to have a comparable P adsorption capacity.

Table 2
The surface area and pore volume of DWTS and MDWTS

Sample	BET Surface area (m ² ·g ⁻¹)	Pore size (nm)	Pore volume (cm ³ ·g ⁻¹)
DWTS	9.852	12.809	0.032
MDWTS500	15.280	21.086	0.081
MDWTS600	8.085	32.315	0.065
MDWTS700	7.386	20.446	0.038
MDWTS800	3.281	35.385	0.029
MDWTS900	3.594	28.571	0.026

Table 1
The chemical oxide content of DWTS and MDWTS

Content (wt% dry)	Elements as an oxide							
	SiO ₂	Al ₂ O ₃	Fe ₂ O ₃	K ₂ O	CaO	Other metal oxide	%WL	Si/Al ratio
DWTS	52.61	13.47	18.71	5.10	6.52	3.6	–	3.91
MDWTS500	57.63	15.49	12.78	4.51	5.93	3.51	11.2	3.72
MDWTS600	56.66	15.22	14.58	4.49	5.83	3.21	13.7	3.72
MDWTS700	57.68	12.60	15.12	4.55	5.52	2.95	13.5	4.58
MDWTS800	56.59	15.79	13.57	4.73	6.08	3.22	15.0	3.58
MDWTS900	58.26	15.05	12.83	4.39	5.79	3.25	16.9	3.87

%WL = % Weight loss at the corresponding temperature.

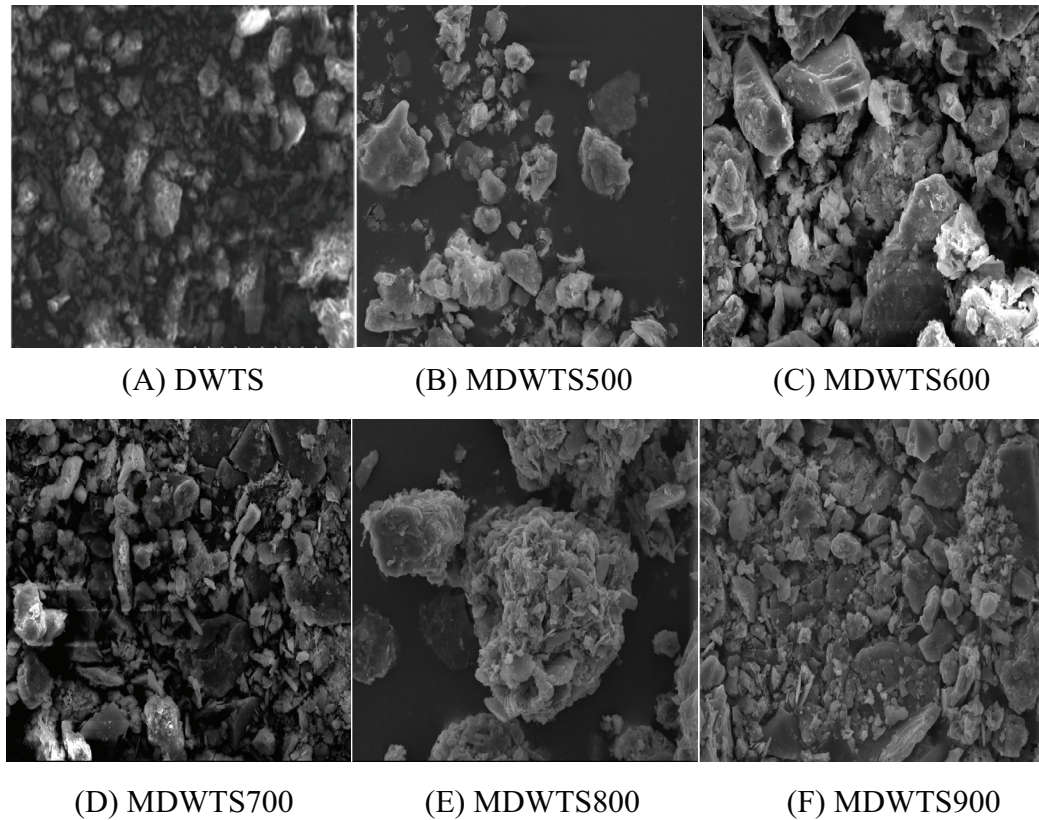


Fig. 1. SEM analysis of DWTS and MDWTS.

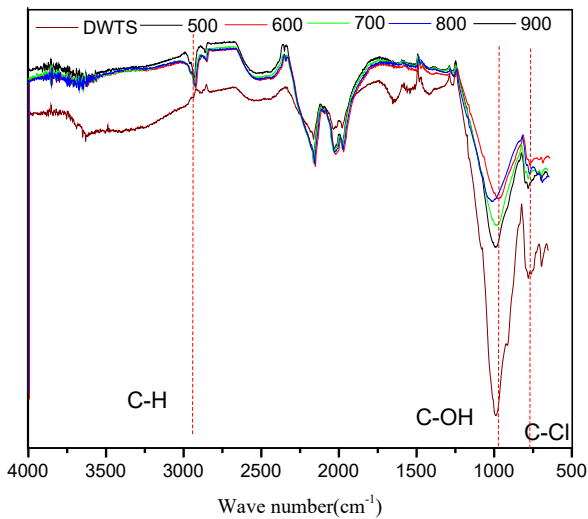


Fig. 2. FTIR analysis of DWTS and MDWTS before adsorption.

In order to analyze the isotherm data, the Langmuir and Freundlich models were used to fit the isotherm data. The results are illustrated in Table 3. The maximum phosphorus adsorption capacity of DWTS (8.87 mg/g) and MDWTS (56.18 mg/g) obtained from Langmuir parameter were a little higher than the experimental data. Meanwhile, Freundlich models (R^2 values were in the range 0.980–0.992) was better fit than Langmuir models (R^2 values were in the range

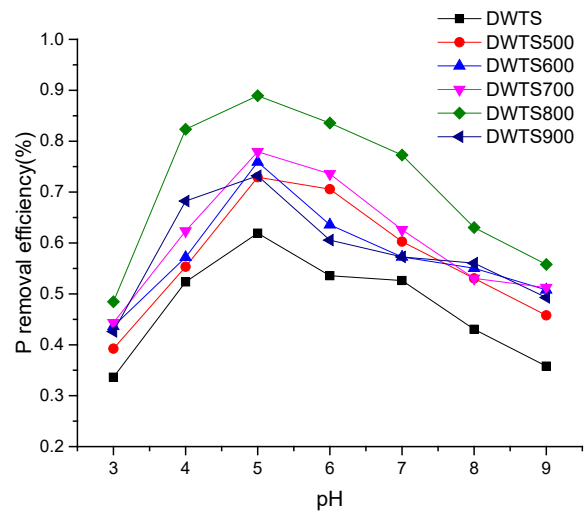


Fig. 3. P adsorption at different P initial concentration using a dosage of 0.1 g DTWS and MDTWS.

0.945–0.989) to describe the adsorption isotherms process which indicated that the adsorption of phosphorus was a heterogeneous surface adsorption process. The Freundlich k_f was related to the affinity of DWTS and MDWTS for P. The fact that a greater k_f value was obtained after modified suggested greater mobility of the aluminum ions towards phosphorus ions, thus influenced the degree of affinity.

Table 3
Isotherms parameters of the Langmuir and Freundlich models

Objective	Experiment	Langmuir parameter			Freundlich		
	q_e (mg/g)	q_{max} (mg/g)	k_L (L/mg)	R^2	k_F	$1/n$	R^2
DWTS	6.50	8.87	0.047	0.989	1.12	0.44	0.992
MDWTS500	12.33	16.95	0.045	0.982	2.11	0.44	0.988
MDWTS600	16.10	25.38	0.031	0.971	1.77	0.56	0.981
MDWTS700	20.43	38.17	0.021	0.976	1.46	0.67	0.983
MDWTS800	25.32	56.18	0.015	0.945	1.34	0.74	0.980
MDWTS900	19.51	38.02	0.019	0.972	1.27	0.69	0.983

Table 4
Fitting results of adsorption kinetics data

Objective	Pseudo first-order				Pseudo-second order			
	q_e (mg/g)	k_1 (1/h)	R^2	SSE	q_e (mg/g)	k_2 (1/h)	R^2	SSE
DWTS	6.00	1.53	0.953	1.64	6.70	0.35	0.967	1.12
MDWTS 500	23.25	2.91	0.987	6.57	24.66	0.24	0.996	2.14
MDWTS 600	29.29	2.18	0.984	12.27	31.69	0.12	0.993	5.50
MDWTS 700	35.50	2.08	0.986	16.55	38.56	0.09	0.992	8.49
MDWTS 800	50.06	2.07	0.987	30.08	54.41	0.07	0.993	16.29
MDWTS 900	42.38	2.30	0.988	19.22	45.68	0.09	0.995	7.88

Meanwhile, the n values which was greater than that in all cases indicated that the adsorption of P onto the DWTS and MDWTS represented good adsorption.

Higher value of Langmuir constant and Freundlich adsorption capacity further reflected the improved strength and affinity of MDWTS for P. Meanwhile, it could be seen that the increase of pyrolysis temperature was benefit for the phosphorus adsorption. The maximum adsorption capacity of P was obtained at 800°C. The influence of pyrolysis temperature on the P adsorption capacity of MDWTS were reflected on the two aspects: (1) the weight loss of DWTS after pyrolysis caused the micropore forming and enlarged the pore size which promoted the adsorption of phosphorus; (2) with the increase of pyrolysis temperature, the ferro-aluminum crystals was formed which was not benefit for the adsorption of phosphorus. Studies have shown that the phosphorus adsorption capacity of DWTS was directly proportional to the content of amorphous ferro-aluminum [17]. The combination of the above two mechanisms made MDWTS800 have the maximum adsorption capacity.

3.2.2. Effect of solution pH on P adsorption

The cases of P adsorption at different solution pH value were shown in Fig. 4(A). It indicated that the adsorption capacity of DWTS and MDWTS was strongly dependent on solution pH. pH increased from 3.0 to 5.0 remarkably increased the P adsorption efficiency. While pH increased from 5.0 to 9.0 remarkably decreased the P-adsorption efficiency. The maximum P adsorption efficiency was appeared at pH 5. The surface charge of the alum sludge can be affected by pH which may change from positive to negative. When alum sludge is added to water, it is surrounded

by the water molecules (H-O-H) on its surface. The positive charge on the alum sludge will weaken the forces holding the protons (H⁺) to the oxygen which make the protons easy to release. The release of H⁺ causes the decrease of pH which leads to a hydroxylated surface of the alum sludge. The surface hydroxyl groups can take part in complexation reactions with metal ions and ligands. Hence, low pH was benefit for the adsorption of phosphorus which had been verified by the experiment results. With the increase of pH, more and more -OH adsorbed on the surface of alum sludge lead to the formation of a new charged counter-ion layer and caused a lower affinity to phosphorus of the alum sludge. Meanwhile, OH⁻ will compete with phosphorus for the active sites which will restrain the adsorption capacity of the alum sludge. Therefore, the adsorption of phosphorus is favored by low pH values and the adsorption capacity will be higher at low pH values than at high pH values. This was agreed with the report of Kim et al. who investigated the effect of pH on phosphorus adsorption and found that a lower pH being favorable to phosphorus adsorption [26]. The pH at the point of zero charge (pHpzc) was also important for P adsorption. The DWTS and MDWTS used in this study had a pHpzc over 8.1. When pH was below the pHpzc, the surface of DWTS and MDWTS would be positively charged which was benefit for electrostatic and chemical reaction to adsorb more P onto the positively charged surface. While with the pH increasing, the surface become negatively charged due to competitive adsorption of OH⁻ which resulted in the decrease of phosphate adsorption.

In a word, it could be seen that the P-adsorption efficiency was greatly increased after modified compared with DWTS. MDWTS800 had a maximum P adsorption efficiency of 89% compared with the others.

3.2.3. Effect of dosage on P adsorption

Fig. 4B shows the effect of adsorbent dosage on the P removal. Both the P-adsorption capacity of DWTS and MDWTS decreased with the increase of the adsorbent dosage. This was consistent with the expectation that higher adsorbent dosages would result in lower adsorption capacity, as the adsorbed phosphorus was distributed among more available binding sites. The P-adsorption capacity decreased from 7.47 mg/g to 1.74 mg/g with the increase of DWTS dosage from 0.5 to 3.0 g/100 ml. The influence of dosage on the P-adsorption capacity among the MDWTS was not obvious which decreased from a range of 17.98 mg/g–22.45 mg/g at a dosage of 0.5 g/100 ml to a range of 3.25 mg/g–3.78 mg/g at a dosage of 3.0 g/100 ml. A negligible decrease of P-adsorption capacity was observed when the dosage was higher than 2.5 g/100 ml. A high-adsorbent dosage could effectively decrease the unsaturation of the ion-exchange sites of DWTS and MDWTS, and consequently, the number of such sites per unit mass got reduced which caused comparatively lesser ion exchange at higher adsorbent amounts.

3.2.4. Effect of contact time

In order to establish equilibrium time for maximum adsorption and also investigate the kinetic sorption mechanisms onto DWTS and MDWTS, the P adsorption on the DWTS and MDWTS at initial concentrations of 100 mg/L P was studied as a function of contact time. The effects of contact time on the adsorption of phosphorus are shown in Fig. 4C. Similar trends were observed for DWTS and MDWTS with a rapid adsorption process within the first 30 min. Then the adsorption process became slow and leveled off after 120 min. Thus, for batch studies, a period of 120 min was adequate for adsorption of phosphorus onto sludge surfaces.

In order to evaluate the phosphorus kinetic sorption mechanisms onto DWTS and MDWTS, the pseudo first-order [Eq. (5)] and pseudo-second order kinetic model [Eq. (6)] were applied to interpret the experimental data.

$$\log(q_e - q_t) = \log q_e - \frac{k_1 \cdot t}{2.303} \tag{5}$$

$$\frac{t}{q_t} = \frac{1}{k_2 q_e^2} + \frac{t}{q_e} \tag{6}$$

where q_t and q_e (mg/g) are the amount of phosphorus adsorbed at time t and at equilibrium time, respectively, and k_1 (1/h) and k_2 (1/h) are the rate constants for the pseudo first-order and pseudo second-order kinetics, respectively. The kinetic parameters, including correlation coefficients (R^2), k_1 and k_2 are determined through linear regression.

Both the two models could describe the adsorption process ($R^2 > 0.95$). The values of q_e were in good agreement with the experimental values. While the pseudo-second order equation gave a slight better fit to the experimental kinetic data than the pseudo-first order model based on the obtained correlation coefficients (R^2) and SSE (sum of squares due to error). This suggested that the adsorption process of phosphorus was a complicated process which included the chemisorption, diffusion/ion exchange, sur-

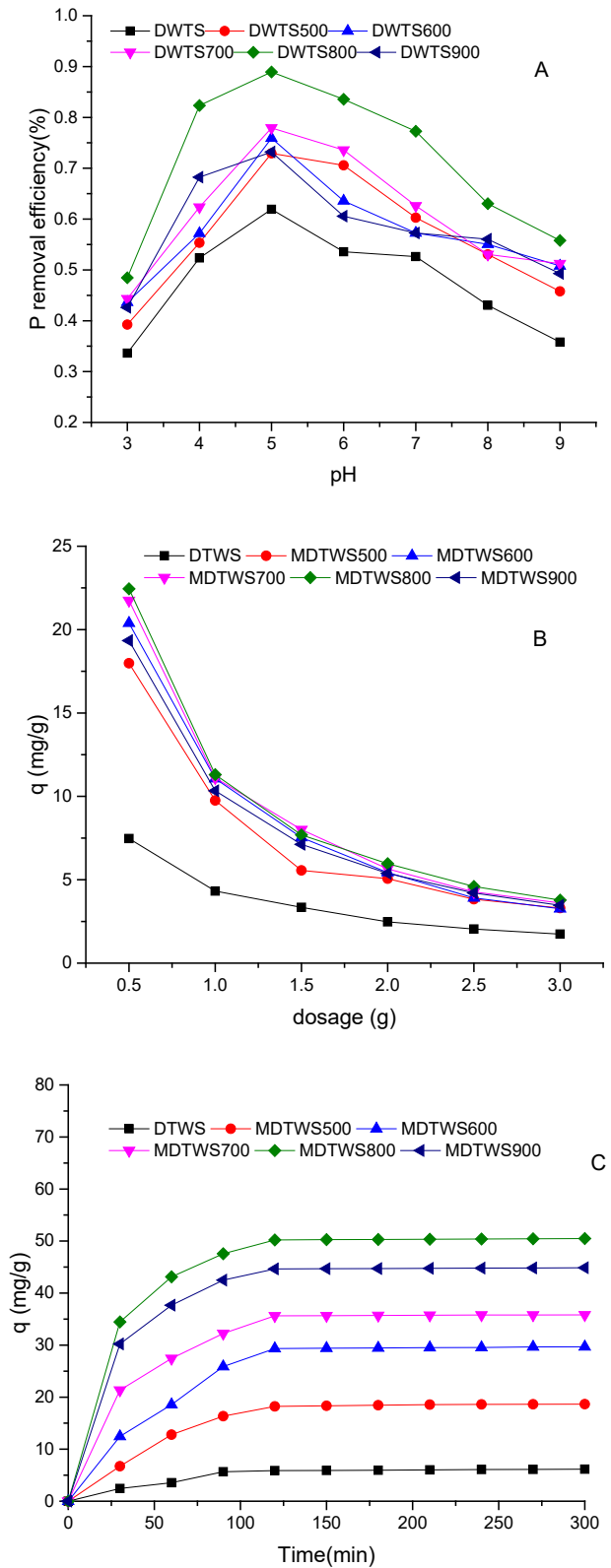
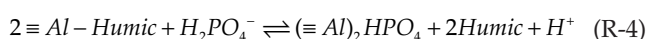
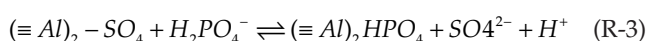
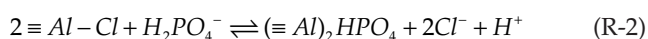
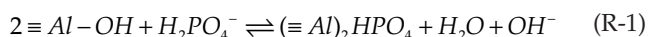


Fig. 4. (A), (B) and (C) effect of pH, dosage and contact time on P adsorption. Note: (A): Effect of pH on adsorption of phosphate using a dosage of 0.1 g DTWS and MDWTS; (B): The effect of DWTS and MDWTS dosage on the P removal; (C): Effect of contact time on P adsorption adsorbed by DTWS and MDWTS.

face adsorption and internal diffusion of particles. The adsorption process could be divided into two steps: rapid adsorption and slow adsorption. The Al-based sludge after pyrolyzed was a kind of porous material which was similar to the activated carbon. At the beginning of rapid adsorption process, the adsorption of phosphorus was taken in the first 30 mins. With the prolonged contact time, chemisorption as the rate-limiting step to sorption made the adsorption reaction rate slow down until reaching the adsorption equilibrium.

3.3. Adsorption mechanism

Ligand exchange action is the main mechanism of phosphorus adsorption by drinking-water treatment sludge. Phosphorus can be adsorbed to the surface of alum sludge through ligand exchange with the active functional groups like $-OH$, $-Cl$, $-SO_4^{2-}$, humic substances (TOC) contained in the alum sludge. The adsorption process could be described by reactions (1)–(4) [27]:



Among the active functional groups, $H_2PO_4^-$ mainly makes ligand exchange with $-OH$. Meanwhile there exists a competition between $H_2PO_4^-$ and $-OH$. The increase of pH will cause the increase of $-OH$ concentration in the solution which will reduce the adsorption capacity of sludge. At the same time, the increase of pH can reduce the positive charge on the adsorbent surface. The increase of negative charge will make repulsion for $H_2PO_4^-$. Therefore, low pH is benefit for the adsorption of phosphorus by the sludge which was consistent with the experimental results.

Although ligand-exchange is an important mechanism for the adsorption mechanism of phosphorus onto the alum sludge, humic substances will compete the surface site with phosphorus which will limit the adsorption capacity of alum sludge. The humic substances are decomposed and converted into solid (biochar), liquid (bio-oil) and gaseous products through pyrolysis which will greatly improve the adsorption sites of alum sludge for the adsorption of phosphorus. Meanwhile, the solid product biochar after pyrolysis is a porous, carbonaceous material which can be used as adsorbents.

The FTIR spectra results of DWTS and MDWTS at various temperatures confirmed the above opinion (Fig. 5). Peaks at $980-1000\text{ cm}^{-1}$ of MDWTS sample were weaker than that of DWTS after adsorption of phosphorus, suggesting pyrolysis can increase the ability of ligand exchange of phosphorus with $-OH$. The weight loss rate was also increased with the pyrolysis temperature when the pyrolysis temperature rose from 500 to 900°C (Table 1), which illustrated that some humic substance (OC) was decomposed during the pyrolysis process, especially at higher temperature.

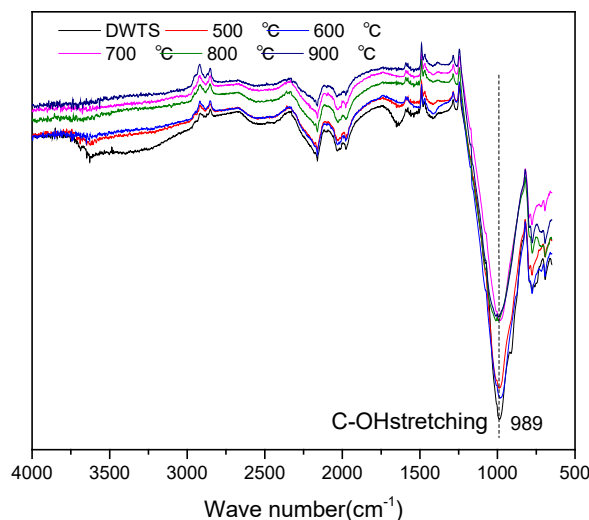


Fig. 5. FTIR spectra of DWTS and MDWTS at various temperatures after adsorption.

3.4. Regeneration of adsorbent

The results of MDWTS800 after regeneration are shown in Fig. 6. The maximum regeneration rate (49%) was obtained at 1.0 mol/L HNO_3 . Low concentration of HNO_3 cannot provide enough nitrate ions for phosphorus exchange adsorbed on MDWTS.

With the increase of HNO_3 concentration, the solution could provide more ions for phosphorus exchange which resulted in an increase of the number of active sites on MDWTS and its re-adsorption capacity of phosphorus. When the HNO_3 concentration was more 1 mol/L , it could not increase the number of active sites on MDWTS which resulted a relative stable regeneration rate. Meanwhile, with the increase of the regeneration time, the regeneration rate of MDWTS gradually increased first and then decreased slightly. When the desorption time was 10 h , the regeneration rate of MDWTS was the highest. This was because the increase of the regeneration time provided more time for the exchange between nitrate ions in the solution and phosphorus on MDWTS. However, when the active sites on the surface of MDWTS was reached to saturation, it was meaningless to prolong the regeneration time. Hence, the optimal regeneration conditions were 1.0 mol/L HNO_3 and 10 h .

4. Conclusion

This study had demonstrated that the adsorption capacity of Al-based DWTS could be greatly improved through pyrolysis. The optimal condition of adsorption of $PO_4^{3-}\text{-P}$ onto MDWTS was $\text{pH } 5.0$, $0.5\text{ g}/100\text{ ml}$ and 2 h contact time. The adsorption isotherm of P onto the adsorbent was well fitted to the Freundlich model and the maximum adsorption capacity (Q_m) of DWTS and MDWTS was 8.87 mg/g and 56.18 mg/g respectively. Resource utilization of DWTS and improve its capacity as a P adsorbent is feasible and environmental friendly which will develop a new approach for the treatment of such kind of sludge in China in the future for the reuse of it as a low-cost material, rather than

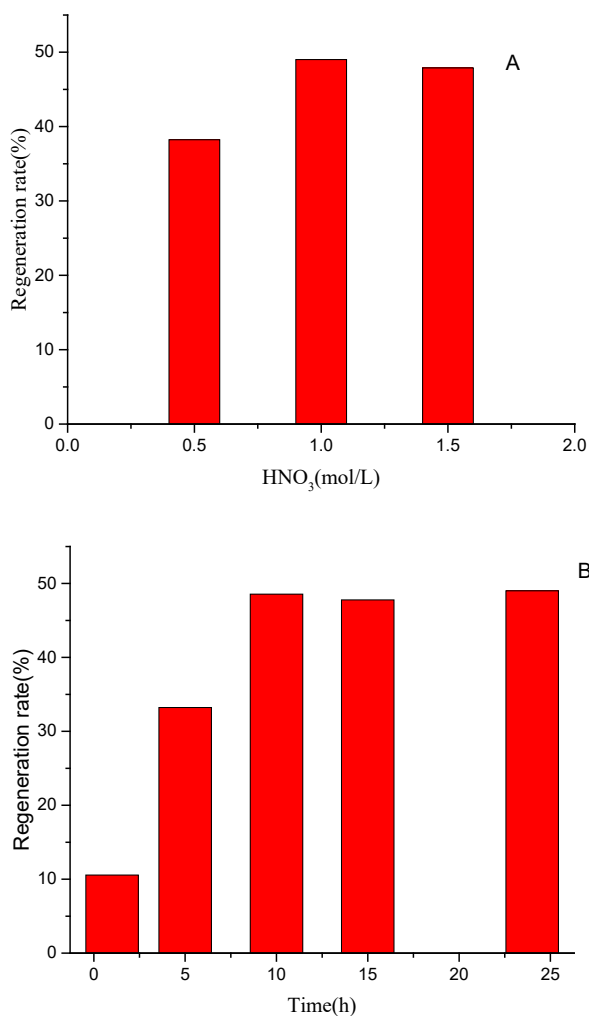


Fig. 6. The influence of HNO₃ concentration and regeneration time on the regeneration of MDWTS800.

as a waste requiring costly disposal, in accordance with the concept of sustainable development.

Acknowledgements

The authors would acknowledge the financial provided by Natural Science Foundation of Hubei Province (2018CFB280), Hubei province scientific research projects (Q20171710), the outstanding youth project of WuHan Polytechnic University (2018J03), and Hubei Important Project of Technological Innovation (2018ABA094).

References

- [1] A. Genz, A. Kornmüller, M. Jekel, Advanced phosphorus removal from membrane filtrates by adsorption on activated aluminium oxide and granulated ferric hydroxide, *Water Res.*, 38 (2004) 3523–3530.
- [2] K. Fytianos, E. Voudrias, N. Raikos, Modelling of phosphorus removal from aqueous and wastewater samples using ferric iron, *Environ. Pollut.*, 101 (1998) 123–130.
- [3] A. Roypoirier, P. Champagne, Y. Filion, Bioretention processes for phosphorus pollution control, *Environ. Rev.*, 18 (2010) 159–173.
- [4] J.Y. Hu, S.L. Ong, W.J. Ng, F. Lu, X.J. Fan, A new method for characterizing denitrifying phosphorus removal bacteria by using three different types of electron acceptors, *Water Res.*, 37 (2003) 3463–3471.
- [5] N. Murayama, S. Yoshida, Y. Takami, H. Yamamoto, J. Shibata, Simultaneous removal of NH₄⁺ and PO₄³⁻ in aqueous solution and its mechanism by using zeolite synthesized from coal fly ash, *Separ. Sci. Technol.*, 38 (2003) 113–130.
- [6] A. Ugurlu, B. Salman, Phosphorus removal by fly ash, *Environ. Int.*, 24 (1998) 911–918.
- [7] R.M. Nageeb, E.D.E.T. Ma, S.M. Fadlalla, Adsorption of methylene blue using modified adsorbents from drinking water treatment sludge, *Water Sci. Technol.*, 74 (2016) 1885.
- [8] S.E. Da, D.M. Morita, A.C. Lima, L.G. Teixeira, Manufacturing ceramic bricks with polyaluminum chloride (PAC) sludge from a water treatment plant, *Water Sci. Technol.*, 71 (2015) 1638–1645.
- [9] M. Xie, Q. Shen, X. Liu, F. Li, D. Gao, Utilization of drinking-water treatment sludge in the manufacturing of ceramic tiles, *Energy Educ. Sci. Technol. Part A: Energy Sci. Res.*, 29 (2012) 267–276.
- [10] J. Liang, C. Wang, Y. Pei, Use of drinking-water treatment sludge for pre-treatment of livestock wastewater, *Chinese J. Environ. Eng.*, 9 (2015) 2569–2576.
- [11] Z. Zhou, Y. Yang, X. Li, Effects of ultrasound pretreatment on the characteristic evolutions of drinking water treatment sludge and its impact on coagulation property of sludge recycling process, *Ultrason. Sonochem.*, 27 (2015) 62–71.
- [12] L. Meng, Y. Chan, H. Wang, Y. Dai, X. Wang, J. Zou, Recycling of iron and silicon from drinking water treatment sludge for synthesis of magnetic iron oxide@SiO₂ composites, *Environ. Sci. Pollut. Res.*, 23 (2016) 5122.
- [13] L. Yang, Y.X. Han, D.T. Wang, High efficiency aluminum coagulant recovery from drinking water treatment plant sludge by using ultrasound assisted acidification, *Adv. Mater. Res.*, 777 (2013) 60–64.
- [14] M. Razali, Y.Q. Zhao, M. Bruen, Effectiveness of a drinking-water treatment sludge in removing different phosphorus species from aqueous solution, *Separ. Purif. Technol.*, 55 (2007) 300–306.
- [15] J. Tie, C. Dong, X. Li, X. Zhu, Phosphorus Adsorption Characteristics of Alum and Iron Sludge from Drinking-Water Treatment Works, in: *International Conference on Bioinformatics and Biomedical Engineering*, 2010, pp. 1–3.
- [16] J.A. Ippolito, K.A. Barbarick, D.M. Heil, J.P. Chandler, E.F. Redente, Phosphorus retention mechanisms of a water treatment residual, *J. Environ. Qual.*, 32 (2003) 1857–1864.
- [17] K. Rubin, Andrej Pohar, V.D.B.C. Dasireddy, B. Likozar, Synthesis, characterization and activity of CuZnGaOx catalysts for the water–gas shift (WGS) reaction for H₂ production and CO removal after reforming, *Fuel Process. Technol.*, (2018) 217–225.
- [18] A.O. Babatunde, Y.Q. Zhao, A.M. Burke, M.A. Morris, J.P. Hanrahan, Characterization of aluminium-based water treatment residual for potential phosphorus removal in engineered wetlands, *Environ. Pollut.*, 157 (2009) 2830.
- [19] A.I. Omoike, G.W. Vanloon, Removal of phosphorus and organic matter removal by alum during wastewater treatment, *Water Res.*, 33 (1999) 3617–3627.
- [20] C. Fang, T. Zhang, P. Li, R.F. Jiang, Y.C. Wang, Application of magnesium modified corn biochar for phosphorus removal and recovery from swine wastewater, *Int. J. Environ. Res. Public Health*, 11 (2014) 9217–9237.
- [21] J. Pan, G. Li, Z. Chen, X. Chen, W. Zhu, K. Xu, Alternative block polyurethanes based on poly(3-hydroxybutyrate–4-hydroxybutyrate) and poly(ethylene glycol), *Biomaterials*, 30 (2009) 2975–2984.
- [22] M. Inyang, B. Gao, W. Ding, P. Pullammanappallil, A.R. Zimmerman, X. Cao, Enhanced lead sorption by biochar derived from anaerobically digested sugarcane bagasse, *Separ. Sci. Technol.*, 46 (2011) 1950–1956.

- [23] C. Barca, C. Gérente, D. Meyer, F. Chazarenc, Y. Andrès, Phosphate removal from synthetic and real wastewater using steel slags produced in Europe, *Water Res.*, 46 (2012) 2376–2384.
- [24] S.G. Lu, S.Q. Bai, L. Zhu, H.D. Shan, Removal mechanism of phosphate from aqueous solution by fly ash, *J. Hazard. Mater.*, 161 (2009) 95–101.
- [25] Q. Guan, X. Hu, D. Wu, S. Xiao, C. Ye, H. Kong, Phosphate removal in marine electrolytes by zeolite synthesized from coal fly ash, *Fuel*, 88 (2009) 1643–1649.
- [26] M.S. Kim, J.G. Chung, A study on the adsorption characteristics of orthophosphates on rutile-type titanium dioxide in aqueous solutions, *J. Colloid Interface Sci.*, 233 (2001) 31–37.
- [27] C. Liu, Y. Yang, N. Wan, Characteristic and mechanisms of chromium(VI) adsorption on alum sludge, *Chinese J. Environ. Eng.*, 7 (2013) 97–102.